Multimodality Imaging in the Diagnosis and Assessment of Cardiac Amyloidosis

Jyothirmayi Velaga[1] Charlene Liew[2] Angeline Choo Choo Poh[2] Phong Teck Lee[4] Narayan Lath[1] Shoen Choon Low[1] Pushan Bharadwaj[3]

[1] Department of Diagnostic Radiology, Singapore General Hospital, Singapore, Singapore
[2] Department of Radiology, Changi General Hospital, Singapore, Singapore
[3] Department of Nuclear Medicine and Molecular Imaging, Singapore General Hospital, Singapore
[4] National Heart Centre, Singapore, Singapore

Address for correspondence Jyothirmayi Velaga, MBBS, DNB, FRCR, FRANZCR, #08-04, 370G Alexandra Road, Singapore 159960, Singapore (e-mail: vjyotirmayi@gmail.com).

World J Nuclear Med 2022;21:173–183.

Abstract

Amyloidosis is a rare disorder where abnormal protein aggregates are deposited in tissues forming amyloid fibrils, leading to progressive organ failure. Although any organ can be affected, cardiac involvement is the main cause of morbidity and mortality associated with amyloidosis as diagnosis is often delayed due to the indolent nature of the disease in some forms. An early diagnosis of disease and knowledge of the type/subtype of cardiac amyloidosis (CA) are essential for appropriate management and better outcome. Echocardiography is often the first line of investigation for patients suspected of CA and offers superior hemodynamic assessment. Although cardiovascular magnetic resonance (CMR) imaging is not diagnostic of CA, it provides vital clues to diagnosis and has a role in disease quantification and prognostication. Radiolabeled bone seeking tracers are the mainstay of diagnosis of CA and when combined with screening of monoclonal light chains, bone scintigraphy offers high sensitivity in diagnosing transthyretin type of CA. This review aims to describe the noninvasive imaging assessment and approach to diagnosis of patients with suspected CA. Imaging features of echocardiography, nuclear scintigraphy, and CMR are described with a brief mention on computed tomography.

Keywords

- cardiac amyloidosis
- strain imaging
- bone scintigraphy
- ^{99m}Tc pyrophosphate (PYP)
- cardiac magnetic resonance
- T1 mapping
- late gadolinium enhancement
- extracellular volume fraction
- myocardial strain
- cardiac computed tomography

Introduction

Amyloidosis is a rare disorder where abnormal proteins are first misfolded and then deposited in tissues as highly ordered aggregates forming amyloid fibrils, leading to progressive organ failure. Amyloid deposition can occur in any organ but the commonly involved organs are heart, lungs, liver, kidneys, bones, skin, or nerves. While there are over 30 different types of amyloid fibril proteins, cardiac amyloidosis (CA) is commonly associated with two types of proteins namely, monoclonal light chain (AL) and transthyretin (ATTR) amyloid proteins (►**Table 1**).[1] ATTR CA is further

DOI https://doi.org/10.1055/s-0042-1751057.
ISSN 1450-1147.

Thieme Medical and Scientific Publishers Pvt. Ltd., A-12, 2nd Floor, Sector 2, Noida-201301 UP, India

Table 1 Common types of amyloidosis (original)

Type	Precursor	Distribution	Acquired/Hereditary	Management
AL	Immunoglobulin light chain	Systemic/Localized	Acquired/hereditary	Chemotherapy, stem cell transplantation
ATTR	Transthyretin wild type	Systemic	Acquired	Liver transplantation TTR stabilizers
	Transthyretin variants	Systemic	Hereditary	TTR stabilizers

Abbreviations: AL, light chain; ATTR, transthyretin amyloidosis.

classified as hereditary or acquired. The acquired form is known as wild type ATTR (ATTRwt) that was previously thought to be confined to elderly men; however, higher prevalence in women has been recently reported in a study by González-López et al.[2] ATTRwt almost exclusively affects the heart and is often associated with carpal tunnel syndrome and lumbar canal stenosis.[3–5] In contrast, hereditary ATTR (ATTRv) presents in younger patients and can be associated with either cardiomyopathy (familial amyloidotic cardiomyopathy, FAC) or neuropathy (familial amyloidotic polyneuropathy, FAP). In contrast, extracardiac manifestations are more common in AL type of CA.[6]

Cardiac involvement is the main cause of morbidity and mortality associated with amyloidosis. Diagnosis is often

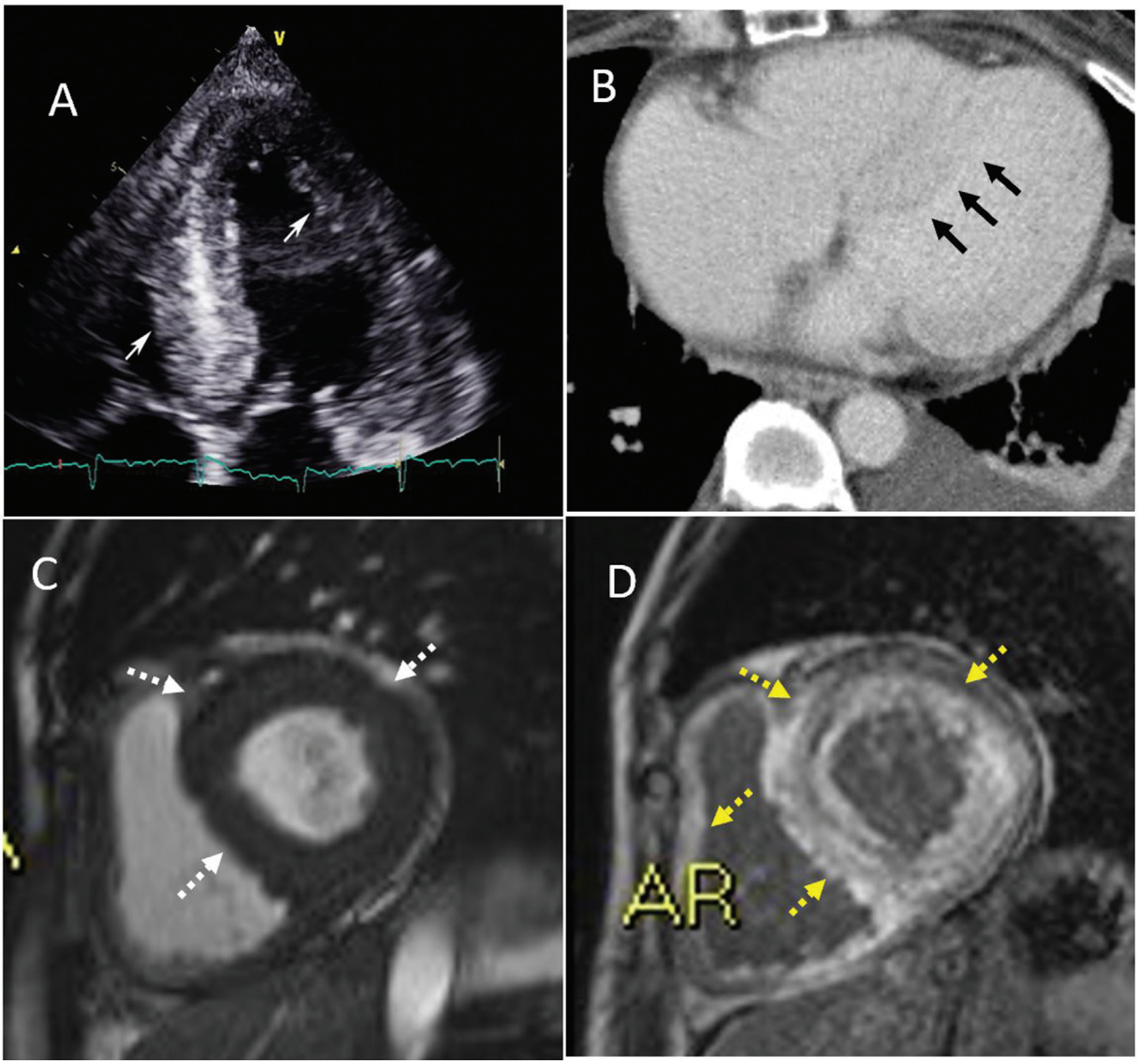

Fig. 1 A 64-year-old woman with amyloid deposition on gastric biopsy. (**A**) Echocardiography shows biventricular hypertrophy (*solid white arrows*) and atrial fibrillation. (**B**) Axial contrast-enhanced computed tomography shows left ventricular hypertrophy (*solid black arrows*). (**C** and **D**) cardiovascular magnetic resonance reveals concentric left ventricular hypertrophy (*dashed white arrows* in **C**) and diffuse transmural myocardial enhancement of ventricles (*dashed yellow arrows* in **D**).

delayed due to the indolent nature of the disease in some forms. The cardiac presentation can range from asymptomatic increase in ventricular wall thickness to severe rapidly progressive heart failure.[6–9] Other clues for cardiac involvement include persistent low-level elevation in serum troponin, discordance between QRS voltage on electrocardiogram and wall thickness on imaging (►**Fig. 1**), unexplained atrioventricular block or prior pacemaker insertion, unexplained atrial or ventricular wall thickening, and family history of cardiomyopathy.[8]

The gold standard for establishing CA deposition is an endomyocardial biopsy (EMB) with Congo red histology demonstrating the pathognomonic apple-green birefringence under polarized light. The limitations of EMB are availability of expertise, complications, errors in tissue processing and unsuitability for quantification. The main advantage of histology is typing of the precursor protein that is essential prior to treatment. With newer treatment options being available, especially for TTR subtype, there is a need to provide information on the CA subtype, extent of disease involvement for prognostication, and assessment of treatment response.[8–10] Advances in cardiac imaging have led to early identification and improved diagnostic confidence of CA for ATTR and have a role in disease quantification and prognostication. This review aims to describe imaging assessment and approach to diagnosis in clinically suspected CA.

Echocardiography

Echocardiography is the first line of screening in patients with suspected CA. CA is characterized by biventricular wall thickening with left ventricular (LV) thickening measuring more than 12 mm in the setting of a nondilated LV (►**Fig. 1A**).[11] The ventricular wall thickening tends to be symmetric in AL and asymmetric in ATTR.[2] The ventricular wall thickening is more prominent in ATTR at diagnosis than in patients with AL, which may reflect the early clinical presentation of AL.[12] Abnormal septal morphology is also noted in ATTR.[2] In addition to increased LV wall thickness presence of granular sparkling appearance of the ventricular myocardium, increased thickness of atrioventricular valves or interatrial septum and pericardial effusion are additional diagnostic clues but are not specific for CA.[11] Diastolic dysfunction is the earliest abnormality and may occur before the onset of symptoms. The LV systolic function is often preserved until the advanced stage of the disease and is measured by ejection fraction reflecting radial thickening. Besides radial thickening, strain imaging also enables assessment of other parameters of ventricular contraction, namely circumferential shortening (circumferential strain [CS]) and longitudinal shortening (longitudinal strain [LS]), of which the longitudinal function is typically involved earlier in CA than the radial contraction. Myocardial strain measures deformation of the myocardium as a percentage change in myocardial length from relaxed state to contractile state produced by application of a force. Strain ratio is the rate by which the deformation occurs (deformation or strain per unit time). Myocardial strain imaging in echocardiography is performed by tissue Doppler imaging, two-dimensional speckle tracking echocardiography (STE), and three-dimensional STE. STE is the currently the widest available technique to quantify myocardial deformation.[13,14] The LS of the LV is severely impaired in CA and can provide an indirect evaluation of the extent of amyloid infiltration.[15] Patterns in LS have been reported as increasing diagnostic accuracy for amyloidosis such as ratio of regional LS values (apical:basal strain ratio or relative apical sparing ratio), or left ventricular ejection fraction to global LS (GLS) ratio.[15,16] Abnormal GLS in the mid and basal walls of the LV with normal values in the apex, known as the apical sparing pattern (or "cherry on top" pattern) (►**Fig. 2**), is 93% sensitive and 82% specific in identifying patients with CA.[17] These indices aid in differentiating CA from other causes of LV wall thickening but are not definitively diagnostic of CA. Additionally, although

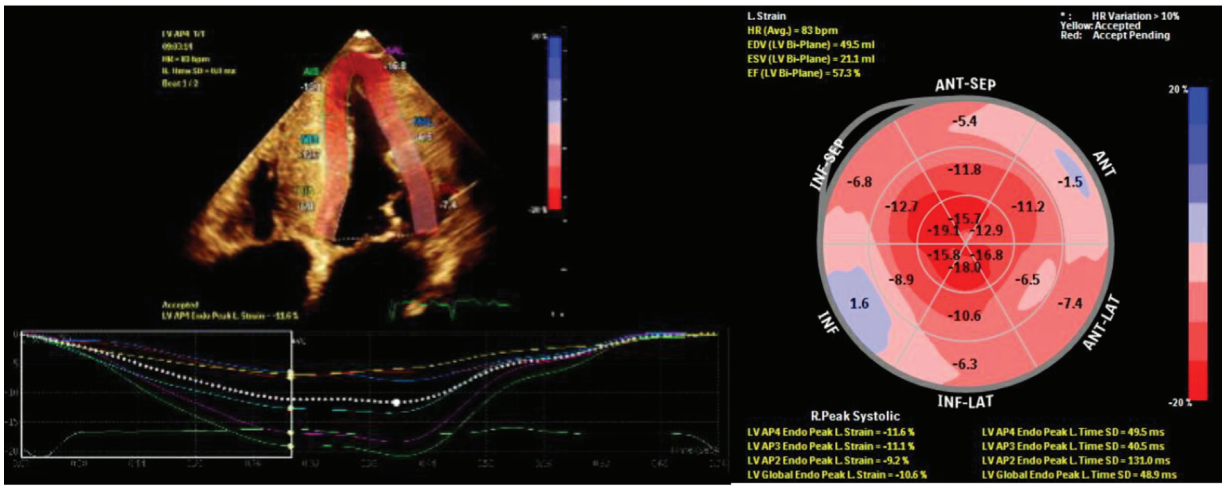

Fig. 2 A 64-year-old patient genopositive for mutant ATTR c.349G > T (p.Ala117Ser). (**A**) Four-chamber view with longitudinal strain map. (**B**) The bullseye longitudinal map of all myocardial segments. Note the reduced global longitudinal strain at −10.6% and apical sparing (> 2:1 apical/basal ratio or "cherry on top") pattern. ATTR, transthyretin amyloidosis.

echocardiographic features of AL-CA and ATTR-CA have been described, echocardiography does not reliably distinguish between the two subtypes, and additional imaging with another modality is often required. Nonetheless, echocardiography remains the superior imaging modality, especially to assess cardiac hemodynamics and diastolic functional assessment that is critical in CA.

Nuclear Medicine

Scintigraphy with Bone Seeking Tracers

Bone seeking tracers are the mainstay of diagnosis of CA. The localization of ^{99m}Tc-disphosphonate to amyloid deposits was first noted by Kula et al in 1977.[18] Currently used bone imaging tracers are ^{99m}Tc pyrophosphate (PYP), ^{99m}Tc 3,3-diphosphono-1,2-propanodicarboxylic acid (^{99m}Tc DPD), and ^{99m}Tc hydroxymethylene diphosphonate (HMDP). There is limited access to ^{99m}Tc DPD and ^{99m}Tc HMDP in the United States and ^{99m}Tc PYP in Europe.[19] Although there is no direct comparison between these tracers, available information suggests that these can be used interchangeably.[19]

Bone seeking tracers can definitively diagnose amyloid type when a plasma cell dyscrasia is excluded and may reliably distinguish CA from its mimics.[20,21] Bone seeking tracers are highly sensitive in detecting early or asymptomatic ATTR type of CA and enable reliable diagnosis of ATTR CA without the need for invasive EMB.[10,21–24] The ability to diagnose ATTR CA noninvasively by bone seeking tracers has rapidly increased the diagnostic utilization of ^{99m}Tc PYP as ATTR CA has become a treatable chronic disease with the approval of tamafidis.[9,25] As treatment options comes at a significant expense, it is crucial to accurately interpret ^{99m}Tc PYP imaging.

Imaging Technique

^{99m}Tc PYP scan needs no specific patient preparation and has no known contraindication to tracer administration. The ^{99m}Tc PYP doses are either readily available as unit doses or as kits for preparation. The radio-pharmaceutical (15–20 mCi) is intravenously injected followed by cardiac or chest (and optional whole body) planar imaging and single-photon positive emission computed tomography (SPECT) after 1 hour of tracer administration.[26] The planar images are obtained in anterior, lateral, and left anterior oblique views acquired for 750,000 counts using a 90 degrees detector configuration with 1.46 zoom factor.[26] The acquisition parameters for SPECT imaging are angular range of 180 degrees, detector configuration of 90 degree with 40 detectors at a zoom factor of one.[26] Delayed SPECT or planar imaging at 3 hours is optional and is recommended if there is persistent blood pool activity on 1 hour images.[26] Recently, Masri et al showed that if ^{99m}Tc PYP positivity is based on the presence of diffuse myocardial tracer uptake on SPECT, a time-efficient 1 hour protocol has the same diagnostic efficacy as a 3 hours protocol.[27]

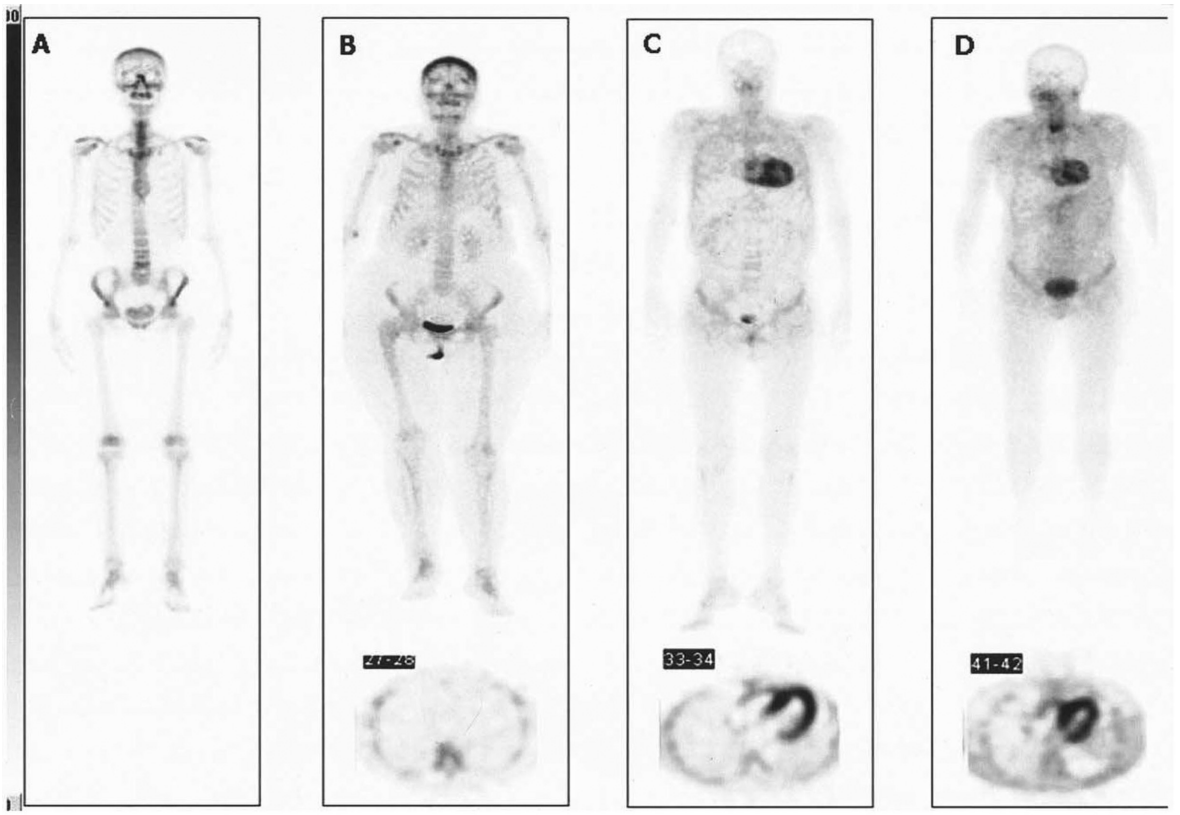

Fig. 3 Spectrum of ^{99m}Tc-3,3-diphosphono-1,2- propanodicarboxylic acid uptake. (**A**) Unaffected control subject without visually detectable uptake. (**B**) Patient with light chain amyloidosis without visually detectable myocardial uptake; mild uptake is visible only at the soft tissue level. (**C** and **D**) Two patients with TTR-related amyloidosis showing strong myocardial uptake with absent bone uptake (reprinted from Perugini et al[28]).

While planar images can be used for visual interpretation and quantification of myocardial uptake, SPECT gives further information on the distribution of the tracer uptake. SPECT is particularly useful in differentiating blood pool uptake from myocardial uptake and assessing myocardial uptake distribution in individuals with positive planar scans. SPECT can also identify regional myocardial differences in uptake and identify uptake in the interventricular septum that is commonly involved in CA. The other advantages of SPECT are its ability to avoid overlap of bone uptake and to quantify the degree of myocardial uptake by comparing to the rib uptake. Whole body planar imaging has the advantage of identifying uptake in other areas of the body beyond the field of view used in cardiac/chest planar imaging (►**Fig. 3**).[28]

Image Interpretation

The patterns of myocardial uptake can be categorized as absent, focal, diffuse, or focal on diffuse. The uptake can be further quantified either by comparing the myocardial uptake with contralateral lung (H/CL ratio) at 1 hour (►**Fig. 4**) or semiquantitatively by comparing to the ribs at 3 hours.

For H/CL assessments, a region of interest (ROI) is drawn over the heart that is then copied and mirrored over the contralateral chest to measure total and absolute mean counts in each ROI. The fraction of heart ROI mean counts to contralateral chest ROI mean counts gives the H/CL ratio. In the presence of visually detectable myocardial uptake on SPECT images, H/CL ratios of more than 1.5 are classified as ATTR positive and ratios below 1.5 as ATTR negative.[23] Semiquantitative method is a visual comparison of myocardial and bone uptake and is scored as grade 0-no uptake, grade 1-less than rib, grade 2-equal to rib, and grade 3-more than rib.[28] A grade of 2 or above is considered positive for semiquantitative assessment, a grade of 1 may either be AL amyloidosis or early ATTR and a negative study can be seen in normal individuals or with AL amyloidosis. Thus, semiquantitative visual score of 2 and above or H/CL ratio more than 1.5 is highly suggestive of ATTR type of CA and can clinch the diagnosis without noninvasive biopsy in the absence of detectable monoclonal protein.[22,23]

Limitations

In some individuals, AL type of CA may be superimposed by ATTR type, especially in elderly individuals, resulting in positive ^{99m}Tc PYP and evidence of plasma cell dyscrasias. EMB would still be required in these cases to exclude AL type of CA. A negative or equivocal ^{99m}Tc PYP scan despite high clinical suspicion of ATTR may also require an EMB to confirm ATTR type of CA. Although highly sensitive for diagnosing ATTR, bone seeking tracers have limited role in disease follow-up and monitoring treatment response.

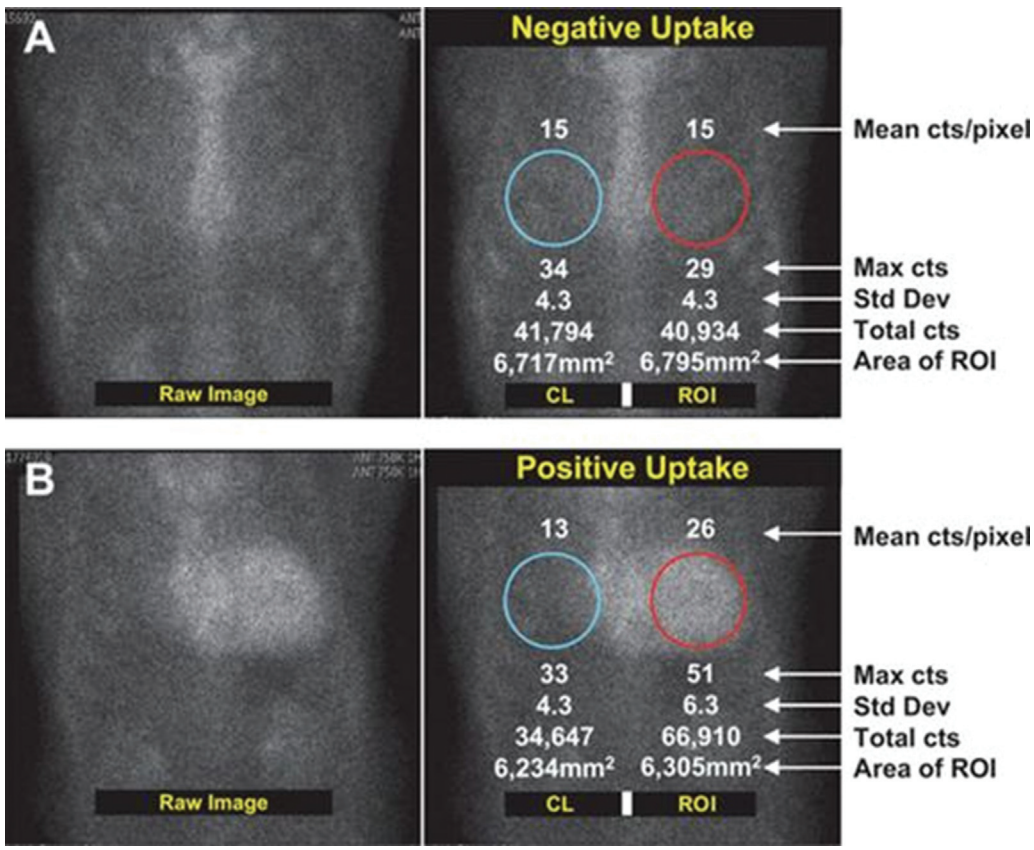

Fig. 4 Raw images of a representative negative (**A**) and positive subject (**B**) are shown 1 hour after radiotracer infusion. ROI circles are depicted in red and the contralateral comparison circle is depicted in blue. C/L, contralateral; Cts, counts; ROI, region of interest; Std Dev, standard deviation (reprinted from from Bokhari et al[23]).

Sympathetic Innervation

Amyloid deposits impair the function of myocardial sympathetic nerve endings and may even lead to sudden death due to fatal arrythmias. The impaired cardiac sympathetic function can be detected in early stages of amyloidosis on I-123 metaiodobenzylguanidine (I-123 MIBG) scintigraphy and in conjunction with cardiac function indices can predict lethal cardiac events and identify the set of patients that can benefit from prophylactic implantable cardioverter-defibrillator implantation.[29–31] I-123 MIBG scintigraphy is analyzed by heart-to-mediastinum activity ratio (HMR) and by cardiac washout ratio that is defined as the percentage change in activity ratio from early to late images. Patients with FAP show significant reduction of MIBG uptake despite preserved LV function and cardiac perfusion. Severity of polyneuropathy correlates inversely with MIBG uptake. Cardiac washout is high in both ATTR and AL patients, whereas the HMR is significantly lower in ATTR.[29] It is not known if patients with ATTRwt or ATTRv FAC without predominant autonomic system dysfunction would benefit from sympathetic innervation imaging and the current role in CA imaging is limited.

Positron Emission Tomography

Fluorodeoxyglucose has limited use in detecting CA as it is difficult to differentiate pathological uptake from physiological uptake.[32] Direct imaging of the amyloid plaques is possible through positron emission tomography imaging using Pittsburgh compound B(11C-PIB), 18F-Florbetaben, and 18F-Florbetapir tracers.[33–36] However, the high cost and limited availability limit the use of these tracers in routine imaging.

I-123 Serum Amyloid P Compound and Technetium-Labeled Aprotinin

I-123 serum amyloid P compound and technetium-labeled aprotinin scintigraphy have role in assessing the whole-body burden of certain types of amyloidosis but their use is limited in CA.[37–40]

Cardiac Magnetic Resonance Imaging

Late Gadolinium Enhancement

The extracellular gadolinium-based contrast agents (GBCA) distribute in the extracellular space of the myocardium but are excluded from the normal myocyte. In CA, the expanded extracellular space retains contrast on delayed imaging that commonly imparts a global pattern of late gadolinium enhancement (LGE) (►**Fig. 1D**).[41] Global LGE is associated with high amyloid burden and markers of systolic and diastolic dysfunction and provides incremental prognostic information.[42,43] The distinct pattern in CA is diffuse global subendocardial LGE, common in AL type (►**Fig. 5**).[44,45] It is also a strong predictor of 1-year mortality in patients with suspected CA.[46] In ATTR, the LGE is more extensive and transmural (►**Fig. 5**).[47] The degree of LGE can also be quantified by query amyloid late enhancement (QALE) score that is an independent predictor of amyloid type (►**Fig. 6**).[47] The total score ranges from 0 (no LGE) to 18 (global transmural LV LGE and RV involvement). The QALE score is higher in ATTR, a score of 13 or above is 82% sensitive and 76% sensitive in differentiating ATTR from AL type.[47] In AL type, a score of 9 or below is associated with better prognosis.[48]

Suboptimal Nulling of the Myocardium

Inversion recovery technique is employed after 10 minutes postcontrast administration to detect LGE.[49] Prior to LGE, incremental inversion times (TI) are applied at mid-ventricular level (TI scout sequence) to determine the optimal TI that nulls the myocardium completely. Normally, after contrast administration the blood pool nulls before myocardium giving good contrast between the myocardium and the blood pool. In CA, increased gadolinium retention in the myocardium shortens the T1 and the myocardium nulls before the blood pool. This suboptimal nulling of the myocardium limits the selection of optimal TI and is a strong predictor of mortality.[50] Loss of temporal nulling of blood pool, myocardium, and spleen in that order in such patients indicates that

Fig. 5 Schematic representation of global subendocardial and transmural patterns of late gadolinium enhancement (LGE) in amyloidosis (*enhancement depicted in white*).

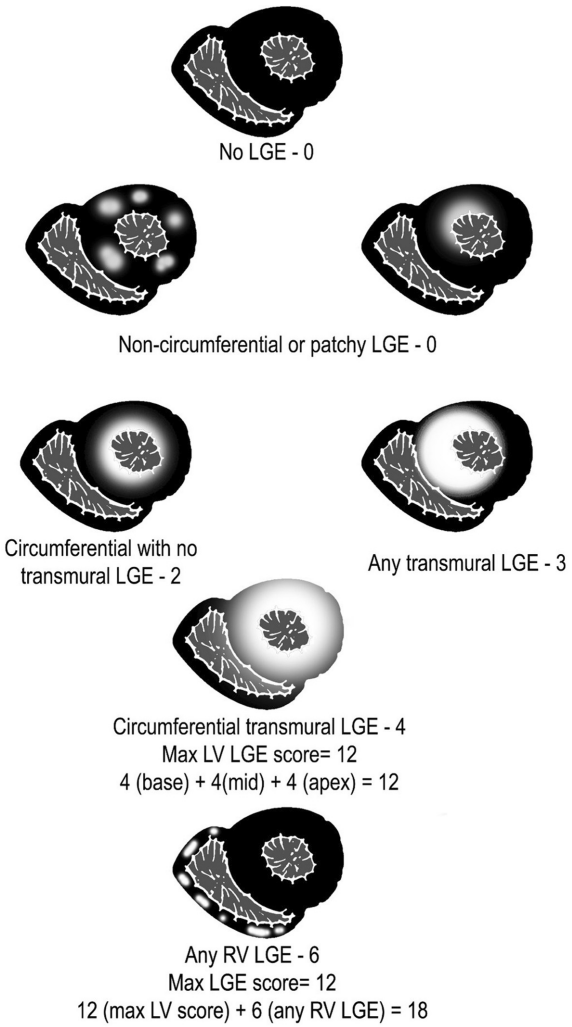

Fig. 6 Schematic representation of query amyloid late enhancement (QALE) score. The QALE score is assessed on late gadolinium enhancement (LGE) images at the level of base, mid, and apex of the ventricles. The highest score is 4 at each level or 6 if right ventricle is involved. The total score ranges from 0 (no LGE) to 18 (global transmural left ventricle (LV) LGE and right ventricle (RV) involvement).

the suboptimal nulling of the myocardium is related to CA rather than technical failure.[51]

Myocardial T1 Mapping

Native T1 mapping quantifies the longitudinal relaxation of tissue without GBCA and can be applied even in patients where GBCA is contraindicated such as in renal failure. A series of images at various inversion times are acquired to derive a T1 recovery curve from which a parametric image that displays T1 relaxation is obtained.[52] T1 values can then be quantified by placing a ROI on the myocardium on the T1 map.[52] Native T1 mapping requires measurement of normal values locally for each scanner configuration.[53,54] On the other hand, postcontrast T1 mapping can be readily incorporated into standard delayed gadolinium enhancement-cardiac magnetic resonance protocols without significant prolongation of study duration.[55] However, it is variable and dependent on various factors such as dosage of contrast administered, time between contrast administration, and image acquisition and renal clearance.[56]

Partition coefficient (λ) is the relationship between changes in pre- and postcontrast myocardium and blood T1 and is calculated by the ratio of the difference of reciprocal values of postcontrast and native T1 of myocardium to that of the blood pool.

$$Partitioncoefficent\ (\lambda) = \frac{\left(\frac{1}{T1myopostGd} - \frac{1}{T1myonative}\right)}{\left(\frac{1}{T1bloodpostGd} - \frac{1}{T1bloodnative}\right)}$$

Extracellular volume (ECV) fraction is obtained from partition coefficient by correcting for hematocrit (λ x [100-hematocrit]) and gives a direct measure of extracellular space reflecting interstitial disease without myocytes.[53,54,57] The native myocardial T1 and the ECV are increased in CA.[58–60] Amyloid deposition is more extensive in ATTR that is reflected as higher ECV than in AL.[61] Despite the higher amyloid volume in ATTR, the native myocardial T1 is lower than in AL. This discordance is probably due to edema in AL that also contributes to the T1 value.[58–60] While both the native myocardial T1 and ECV correlate with indexes of systolic and diastolic function, indexed LV mass, and known prognostic biomarkers, the correlation is stronger with ECV.[61]

Myocardial T2 Mapping

T2 mapping employs similar principle used in T1 mapping where a series of T2-weighted images are applied to obtain T2 decay curve with sequences such as turbo spin echo (TSE) with varying echo time, T2 preparation steady-state free precession (SSFP) sequence, or a sequence scheme that combines spin echo excitation with gradient echo readout.[54] T2 mapping is also a noncontrast sequence and hence can be used in patients with renal failure. However, T2 mapping is prone to confounders such as sensitivity to T1 and off resonance effects.[54] T2 relaxation time increases with increasing water content and is elevated in CA owing to myocardial edema. While myocardial T1 is a measure of combination of amyloid burden and myocardial edema, T2 is more specific for myocardial edema. T2 values are higher in AL than in ATTR and within AL, the values are higher in treatment naïve patients than during or after treatment.[62] It is well known that AL portrays poor survival compared with ATTR and hence myocardial edema is a possible additional mechanism in myocardial damage and predictor for outcome in AL patients.[62]

Myocardial Tagging

Myocardial tagging analyzes deformation or strain of myocardium to quantify LV wall motion abnormalities (►**Fig. 7**). Lines or grids are superimposed on the myocardium at the beginning of a cine sequence and the subsequent deformation of the lines throughout the cardiac cycle is noted that is reduced in CA.[63] CS is shortening in short-axis plane in a direction tangential to epicardial surface. LS is base to apex shortening tangential to the myocardial wall in the long-axis plane. The LS is significantly decreased in CA when compared

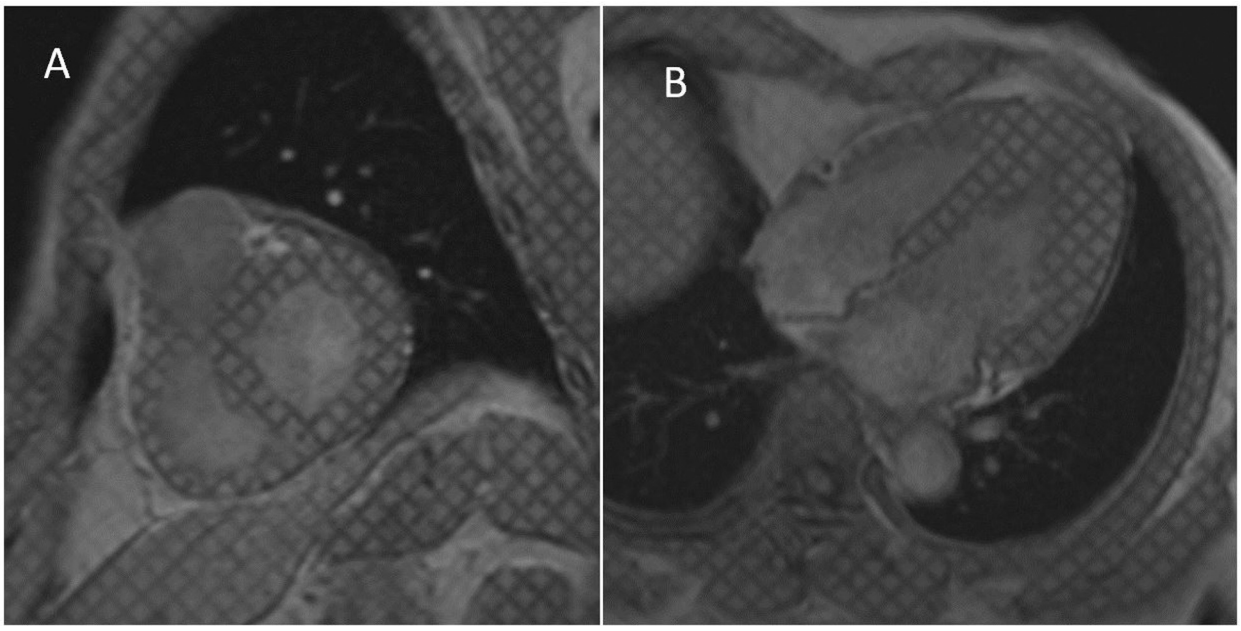

Fig. 7 Cardiovascular magnetic resonance short-axis (**A**) and long-axis (**B**) images through the mid-left ventricle demonstrate application of myocardial tagging at end-diastole. The tag lines are seen as dark lines that deform along with the myocardium during systole.

with hypertrophic cardiomyopathy that is an imaging mimicker of CA, but further studies are needed to establish differentiation from other causes of LV hypertrophy.[64] Prominent base to apex gradient higher at the apical level suggests apical sparing that is known to be specific for CA on echocardiography.[64] Good correlation of CS and LS with positive CA and the quantitative nature of the parameters have a potential for disease detection, quantification of amyloid load, and prognostication.[65]

Cardiac Computed Tomography

The morphological manifestation of myocardial thickening in CA can be appreciated on CT (►**Fig. 1B**).[66] Studies have shown that ECV can also be estimated on conventional as

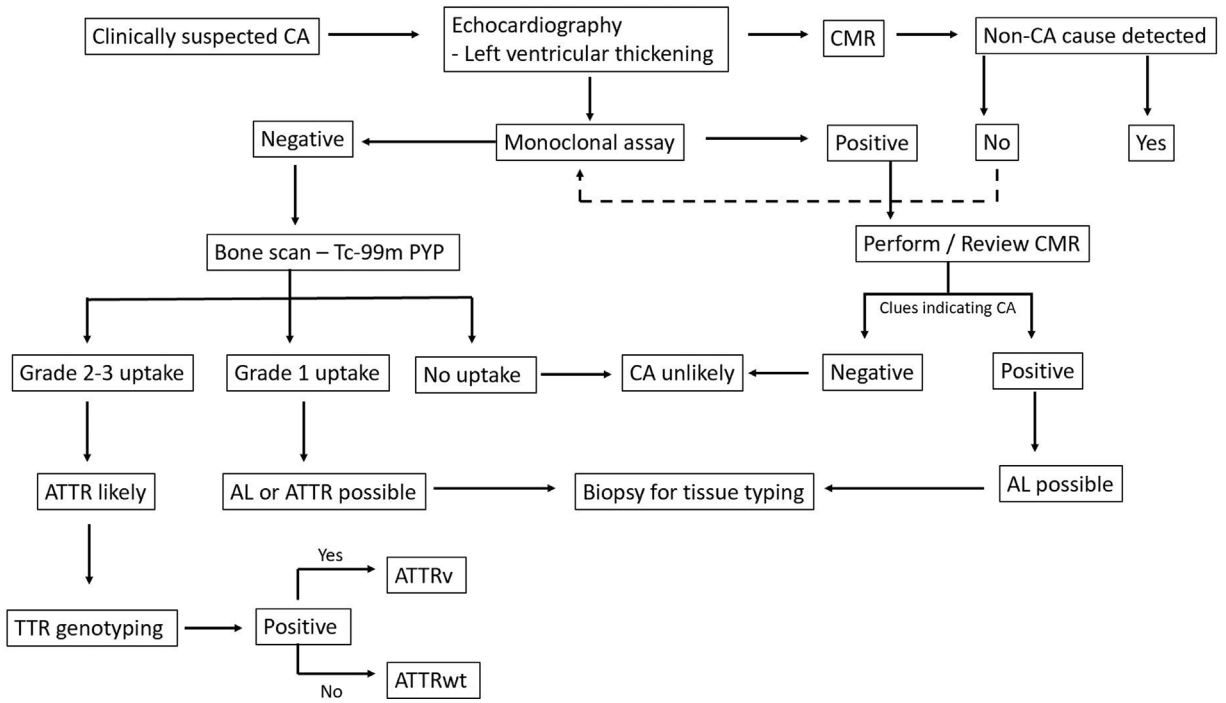

Fig. 8 Diagnostic algorithm in suspected cardiac amyloidosis (CA). Echocardiography is the first line of investigation in clinically suspected patients with CA. Cardiac magnetic resonance imaging (CMR) is not diagnostic but can exclude other causes or direct further biopsy. ATTR is more likely if the monoclonal assay is negative and the bone scintigraphy shows grade 2–3 uptake. A combination of positive monoclonal assay and positive CMR findings can indicate light chain type of CA. ATTR, transthyretin amyloidosis.

well as dual-energy CT.[57,67] However, poor signal to noise ratio compared with cardiac magnetic resonance (CMR) and the use of ionizing radiation limit wider application CT for myocardial tissue characterization.[68] CT may be of value in the subset of patients where magnetic resonance imaging may not be feasible such as in patients with pace makers and claustrophobia.

Diagnostic Approach

In patients with clinically suspected amyloidosis, echocardiography is often the first line of investigation. If echocardiography shows features indicative or suggestive of CA, CMR should be considered as the next line of investigation followed by bone scan. When combined with monoclonal protein detection, there is high diagnostic confidence of bone scan for diagnosing ATTR CA or in ruling out CA. In the absence of monoclonal proteins, a high grade (2 or 3) visual uptake or H/CL ratio more than 1.5 increases the specificity of ATTR amyloidosis, while CA can be deemed unlikely when there is no visual uptake (grade 0). In the former subset of patients, combination of clinical features and echocardiography or CMR findings, diagnosis of ATTR can be established without histological confirmation.[22] Further genotyping is required to differentiate between wild type and variant amyloid, the latter showing TTR gene mutation.[22] For the cases that do not fall into either category, further review or assessment with CMR and/or histological confirmation and amyloid typing may be required for further evaluation. There has been significant progress in the treatment of CA and the therapies are specific for the type of CA. Hence, there is need to diagnose CA at an early stage and to identify the amyloid type. Thus, the goal of the diagnostic algorithm (►**Fig. 8**) is to direct therapeutic options in treating CA.

Conclusion

CA is underrecognized and the diagnosis is often delayed without high index of clinical suspicion. With advances in treatment strategies, it is even more important to detect CA early on in the disease process as the management strategies are more effective before significant cardiac dysfunction. In addition to early detection, it is also pivotal to differentiate between different types of CA as the management approach is tailored to the specific type of CA. The goal of imaging and the diagnostic approach is early detection or ruling of CA and also in early noninvasive diagnosis of ATTR. For equivocal cases and suspected AL type, tissue typing is required. Imaging also plays a vital role in follow-up of these patients to assess treatment response.

Conflict of Interest
None declared.

Acknowledgments
We acknowledge Dr. Kenneth Fu Wen Chin for technical help with the illustrations.

References

1 Sipe JD, Benson MD, Buxbaum JN, et al. Amyloid fibril proteins and amyloidosis: chemical identification and clinical classification International Society of Amyloidosis 2016 Nomenclature Guidelines. Amyloid 2016;23(04):209–213
2 González-López E, Gagliardi C, Dominguez F, et al. Clinical characteristics of wild-type transthyretin cardiac amyloidosis: disproving myths. Eur Heart J 2017;38(24):1895–1904
3 García-Pavía P, Tomé-Esteban MT, Rapezzi C. [Amyloidosis. Also a heart disease]. Rev Esp Cardiol 2011;64(09):797–808
4 Gertz MA, Benson MD, Dyck PJ, et al. Diagnosis, prognosis, and therapy of transthyretin amyloidosis. J Am Coll Cardiol 2015;66 (21):2451–2466
5 Yanagisawa A, Ueda M, Sueyoshi T, et al. Amyloid deposits derived from transthyretin in the ligamentum flavum as related to lumbar spinal canal stenosis. Mod Pathol 2015;28(02):201–207
6 Fikrle M, Paleček T, Kuchynka P, et al. Cardiac amyloidosis: a comprehensive review. Cor Vasa 2013;55(01):e60–e75
7 Rapezzi C, Longhi S, Milandri A, et al. Cardiac involvement in hereditary-transthyretin related amyloidosis. Amyloid 2012;19 (Suppl 1):16–21
8 Kittleson MM, Maurer MS, Ambardekar AV, et al; American Heart Association Heart Failure and Transplantation Committee of the Council on Clinical Cardiology. Cardiac amyloidosis: evolving diagnosis and management: a scientific statement from the American Heart Association. Circulation 2020;142 (01):e7–e22
9 Maurer MS, Schwartz JH, Gundapaneni B, et al; ATTR-ACT Study Investigators. Tafamidis treatment for patients with transthyretin amyloid cardiomyopathy. N Engl J Med 2018;379(11):1007–1016
10 Ruberg FL, Grogan M, Hanna M, Kelly JW, Maurer MS. Transthyretin amyloid cardiomyopathy: JACC state-of-the-art review. J Am Coll Cardiol 2019;73(22):2872–2891
11 Rapezzi C, Merlini G, Quarta CC, et al. Systemic cardiac amyloidoses: disease profiles and clinical courses of the 3 main types. Circulation 2009;120(13):1203–1212
12 Siddiqi OK, Ruberg FL. Cardiac amyloidosis: an update on pathophysiology, diagnosis, and treatment. Trends Cardiovasc Med 2018;28(01):10–21
13 Amzulescu MS, De Craene M, Langet H, et al. Myocardial strain imaging: review of general principles, validation, and sources of discrepancies. Eur Heart J Cardiovasc Imaging 2019;20(06): 605–619
14 Geyer H, Caracciolo G, Abe H, et al. Assessment of myocardial mechanics using speckle tracking echocardiography: fundamentals and clinical applications. J Am Soc Echocardiogr 2010;23(04): 351–369, quiz 453–455
15 Ternacle J, Bodez D, Guellich A, et al. Causes and consequences of longitudinal LV dysfunction assessed by 2D strain echocardiography in cardiac amyloidosis. JACC Cardiovasc Imaging 2016;9 (02):126–138
16 Pagourelias ED, Mirea O, Duchenne J, et al. Echo parameters for differential diagnosis in cardiac amyloidosis: a head-to-head comparison of deformation and nondeformation parameters. Circ Cardiovasc Imaging 2017;10(03):e005588
17 Top RPB-P. 10 Things To Know When Performing Cardiac Imaging to Assess Cardiac Amyloidosis 2020 [Accessed April 8, 2022 from: https://www.acc.org/latest-in-cardiology/articles/2020/02/27/14/47/top-10-things-to-know-when-performing-cardiac-imaging-to-assess-cardiac-amyloidosis
18 Kula RW, Engel WK, Line BR. Scanning for soft-tissue amyloid. Lancet 1977;1(8002):92–93
19 Dorbala S, Ando Y, Bokhari S, et al. ASNC/AHA/ASE/EANM/HFSA/ISA/SCMR/SNMMI expert consensus recommendations for multimodality imaging in cardiac amyloidosis: part 1 of 2-evidence base and standardized methods of imaging. J Nucl Cardiol 2019;26(06):2065–2123

20 Galat A, Rosso J, Guellich A, et al. Usefulness of (99m)Tc-HMDP scintigraphy for the etiologic diagnosis and prognosis of cardiac amyloidosis. Amyloid 2015;22(04):210–220
21 Hutt DF, Quigley AM, Page J, et al. Utility and limitations of 3,3-diphosphono-1,2-propanodicarboxylic acid scintigraphy in systemic amyloidosis. Eur Heart J Cardiovasc Imaging 2014;15(11):1289–1298
22 Gillmore JD, Maurer MS, Falk RH, et al. Nonbiopsy diagnosis of cardiac transthyretin amyloidosis. Circulation 2016;133(24):2404–2412
23 Bokhari S, Castaño A, Pozniakoff T, Deslisle S, Latif F, Maurer MS. (99m)Tc-pyrophosphate scintigraphy for differentiating light-chain cardiac amyloidosis from the transthyretin-related familial and senile cardiac amyloidoses. Circ Cardiovasc Imaging 2013;6(02):195–201
24 Rapezzi C, Quarta CC, Guidalotti PL, et al. Role of (99m)Tc-DPD scintigraphy in diagnosis and prognosis of hereditary transthyretin-related cardiac amyloidosis. JACC Cardiovasc Imaging 2011;4(06):659–670
25 Gerber J, Miller EJ. Optimal interpretation of Tc99m PYP in 2020: avoiding the million-dollar mistake. J Nucl Cardiol 2021;28(02):503–506
26 Dorbala S, Bokhari S, Miller E, Bullock-Palmer R, Soman P, Thompson R. ASNC practice points: 99m-technetium-pyrophosphate imaging for transthyretin cardiac amyloidosis. 2019 (American society of nuclear cardiology website). Accessed September 2021 at: https://www.asnc.org/Files/Amyloid/ASNC%20Practice%20Point-99mTechnetium-Pyrophosphate.2019.pdf
27 Masri A, Bukhari S, Ahmad S, et al. Efficient 1-hour technetium-99 m pyrophosphate imaging protocol for the diagnosis of transthyretin cardiac amyloidosis. Circ Cardiovasc Imaging 2020;13(02):e010249
28 Perugini E, Guidalotti PL, Salvi F, et al. Noninvasive etiologic diagnosis of cardiac amyloidosis using 99mTc-3,3-diphosphono-1,2-propanodicarboxylic acid scintigraphy. J Am Coll Cardiol 2005;46(06):1076–1084
29 Noordzij W, Glaudemans AW, van Rheenen RW, et al. (123)I-Labelled metaiodobenzylguanidine for the evaluation of cardiac sympathetic denervation in early stage amyloidosis. Eur J Nucl Med Mol Imaging 2012;39(10):1609–1617
30 Nagahara D, Nakata T, Hashimoto A, et al. Predicting the need for an implantable cardioverter defibrillator using cardiac metaiodobenzylguanidine activity together with plasma natriuretic peptide concentration or left ventricular function. J Nucl Med 2008;49(02):225–233
31 Coutinho MC, Cortez-Dias N, Cantinho G, et al. Reduced myocardial 123-iodine metaiodobenzylguanidine uptake: a prognostic marker in familial amyloid polyneuropathy. Circ Cardiovasc Imaging 2013;6(05):627–636
32 Lee JH, Lee GY, Kim SJ, et al. Imaging findings and literature review of (18)F-FDG PET/CT in primary systemic AL amyloidosis. Nucl Med Mol Imaging 2015;49(03):182–190
33 Antoni G, Lubberink M, Estrada S, et al. In vivo visualization of amyloid deposits in the heart with 11C-PIB and PET. J Nucl Med 2013;54(02):213–220
34 Dorbala S, Vangala D, Semer J, et al. Imaging cardiac amyloidosis: a pilot study using ^{18}F-florbetapir positron emission tomography. Eur J Nucl Med Mol Imaging 2014;41(09):1652–1662
35 Park MA, Padera RF, Belanger A, et al. 18F-florbetapir binds specifically to myocardial light chain and transthyretin amyloid deposits: autoradiography study. Circ Cardiovasc Imaging 2015;8(08):e002954
36 Law WP, Wang W, Moore P, Mollee P, Ng A. Cardiac amyloid imaging with ^{18}F-florbetaben positron emission tomography: a pilot study. Amyloid 2017;24(Suppl 1):162
37 Hawkins PN, Lavender JP, Pepys MB. Evaluation of systemic amyloidosis by scintigraphy with 123I-labeled serum amyloid P component. N Engl J Med 1990;323(08):508–513
38 Hazenberg BP, van Rijswijk MH, Piers DA, et al. Diagnostic performance of 123I-labeled serum amyloid P component scintigraphy in patients with amyloidosis. Am J Med 2006;119(04):355.e15–355.e24
39 Bokhari S, Shahzad R, Castaño A, Maurer MS. Nuclear imaging modalities for cardiac amyloidosis. J Nucl Cardiol 2014;21(01):175–184
40 Schaadt BK, Hendel HW, Gimsing P, Jønsson V, Pedersen H, Hesse B. 99mTc-aprotinin scintigraphy in amyloidosis. J Nucl Med 2003;44(02):177–183
41 Ordovas KG, Higgins CB. Delayed contrast enhancement on MR images of myocardium: past, present, future. Radiology 2011;261(02):358–374
42 Syed IS, Glockner JF, Feng D, et al. Role of cardiac magnetic resonance imaging in the detection of cardiac amyloidosis. JACC Cardiovasc Imaging 2010;3(02):155–164
43 Boynton SJ, Geske JB, Dispenzieri A, et al. LGE provides incremental prognostic information over serum biomarkers in AL cardiac amyloidosis. JACC Cardiovasc Imaging 2016;9(06):680–686
44 Maceira AM, Joshi J, Prasad SK, et al. Cardiovascular magnetic resonance in cardiac amyloidosis. Circulation 2005;111(02):186–193
45 Vogelsberg H, Mahrholdt H, Deluigi CC, et al. Cardiovascular magnetic resonance in clinically suspected cardiac amyloidosis: noninvasive imaging compared to endomyocardial biopsy. J Am Coll Cardiol 2008;51(10):1022–1030
46 Austin BA, Tang WH, Rodriguez ER, et al. Delayed hyper-enhancement magnetic resonance imaging provides incremental diagnostic and prognostic utility in suspected cardiac amyloidosis. JACC Cardiovasc Imaging 2009;2(12):1369–1377
47 Dungu JN, Valencia O, Pinney JH, et al. CMR-based differentiation of AL and ATTR cardiac amyloidosis. JACC Cardiovasc Imaging 2014;7(02):133–142
48 Wan K, Sun J, Han Y, et al. Increased prognostic value of query amyloid late enhancement score in light-chain cardiac amyloidosis. Circ J 2018;82(03):739–746
49 Kramer CM, Barkhausen J, Flamm SD, Kim RJ, Nagel ESociety for Cardiovascular Magnetic Resonance Board of Trustees Task Force on Standardized Protocols. Standardized cardiovascular magnetic resonance (CMR) protocols 2013 update. J Cardiovasc Magn Reson 2013;15(01):91
50 White JA, Kim HW, Shah D, et al. CMR imaging with rapid visual T1 assessment predicts mortality in patients suspected of cardiac amyloidosis. JACC Cardiovasc Imaging 2014;7(02):143–156
51 Pandey T, Jambhekar K, Shaikh R, Lensing S, Viswamitra S. Utility of the inversion scout sequence (TI scout) in diagnosing myocardial amyloid infiltration. Int J Cardiovasc Imaging 2013;29(01):103–112
52 Hamlin SA, Henry TS, Little BP, Lerakis S, Stillman AE. Mapping the future of cardiac MR imaging: case-based review of T1 and T2 mapping techniques. Radiographics 2014;34(06):1594–1611
53 Moon JC, Messroghli DR, Kellman P, et al; Society for Cardiovascular Magnetic Resonance Imaging Cardiovascular Magnetic Resonance Working Group of the European Society of Cardiology. Myocardial T1 mapping and extracellular volume quantification: a Society for Cardiovascular Magnetic Resonance (SCMR) and CMR Working Group of the European Society of Cardiology consensus statement. J Cardiovasc Magn Reson 2013;15(01):92
54 Messroghli DR, Moon JC, Ferreira VM, et al. Clinical recommendations for cardiovascular magnetic resonance mapping of T1, T2, T2* and extracellular volume: a consensus statement by the Society for Cardiovascular Magnetic Resonance (SCMR) endorsed by the European Association for Cardiovascular Imaging (EACVI). J Cardiovasc Magn Reson 2017;19(01):75
55 Jellis CL, Kwon DH. Myocardial T1 mapping: modalities and clinical applications. Cardiovasc Diagn Ther 2014;4(02):126–137
56 Burt JR, Zimmerman SL, Kamel IR, Halushka M, Bluemke DA. Myocardial T1 mapping: techniques and potential applications. Radiographics 2014;34(02):377–395

57 Treibel TA, Bandula S, Fontana M, et al. Extracellular volume quantification by dynamic equilibrium cardiac computed tomography in cardiac amyloidosis. J Cardiovasc Comput Tomogr 2015;9(06):585–592
58 Karamitsos TD, Piechnik SK, Banypersad SM, et al. Noncontrast T1 mapping for the diagnosis of cardiac amyloidosis. JACC Cardiovasc Imaging 2013;6(04):488–497
59 Fontana M, Banypersad SM, Treibel TA, et al. Native T1 mapping in transthyretin amyloidosis. JACC Cardiovasc Imaging 2014;7(02):157–165
60 Liu JM, Liu A, Leal J, et al. Measurement of myocardial native T1 in cardiovascular diseases and norm in 1291 subjects. J Cardiovasc Magn Reson 2017;19(01):74
61 Fontana M, Banypersad SM, Treibel TA, et al. Differential myocyte responses in patients with cardiac transthyretin amyloidosis and light-chain amyloidosis: a cardiac MR imaging study. Radiology 2015;277(02):388–397
62 Kotecha T, Martinez-Naharro A, Treibel TA, et al. Myocardial edema and prognosis in amyloidosis. J Am Coll Cardiol 2018;71(25):2919–2931
63 Jeung MY, Germain P, Croisille P, El ghannudi S, Roy C, Gangi A. Myocardial tagging with MR imaging: overview of normal and pathologic findings. Radiographics 2012;32(05):1381–1398
64 Williams LK, Forero JF, Popovic ZB, et al. Patterns of CMR measured longitudinal strain and its association with late gadolinium enhancement in patients with cardiac amyloidosis and its mimics. J Cardiovasc Magn Reson 2017;19(01):61
65 Oda S, Utsunomiya D, Nakaura T, et al. Identification and assessment of cardiac amyloidosis by myocardial strain analysis of cardiac magnetic resonance imaging. Circ J 2017;81(07):1014–1021
66 Deux JF, Mihalache CI, Legou F, et al. Noninvasive detection of cardiac amyloidosis using delayed enhanced MDCT: a pilot study. Eur Radiol 2015;25(08):2291–2297
67 Lee HJ, Im DJ, Youn JC, et al. Myocardial extracellular volume fraction with dual-energy equilibrium contrast-enhanced cardiac CT in nonischemic cardiomyopathy: a prospective comparison with cardiac MR imaging. Radiology 2016;280(01):49–57
68 Scully PR, Bastarrika G, Moon JC, Treibel TA. Myocardial extracellular volume quantification by cardiovascular magnetic resonance and computed tomography. Curr Cardiol Rep 2018;20(03):15

